INDIAN JOURNAL OF SCIENCE AND TECHNOLOGY

RESEARCH ARTICLE

Check for updates

OPEN ACCESS

Received: 04-11-2022

Accepted: 17-01-2023

Published: 11-02-2023

Citation: Ramesh K, Ramanathan S, Vinod B (2023) Investigation and Synthesis of Biowaste Composite by Squeeze Casting Process: Microstructure Evolution for Biomedical Applications. Indian Journal of Science and Technology 16(6): 409-419. https://doi.org/10.17485/IJST/v16i6.2137

* **Corresponding author**.

rameshk1981@gmail.com

Funding: None

Competing Interests: None

Published By Indian Society for Education and Environment (iSee)

ISSN
Print: 0974-6846
Electronic: 0974-5645

Investigation and Synthesis of Biowaste Composite by Squeeze Casting Process: Microstructure Evolution for Biomedical Applications

K Ramesh[1]*, S Ramanathan[2], B Vinod[3]

1 Research Scholar, Department of Manufacturing Engineering, Annamalai University, Annamalai Nagar, Chidambaram, 608 002, India
2 Professor, Department of Manufacturing Engineering, Annamalai University, Annamalai Nagar, Chidambaram, 608 002, India
3 Associate Professor, Department of Mechanical Engineering, Siddharth Institute of Engineering & Technology, Puttur, 517583, India

Abstract

Objectives: To investigate the mechanical and microstructural behaviour of zinc hybrid composites. Zinc alloys are utilized in biomaterial development for implant applications due to their suitable corrosion properties. However, the advantages connected with hybrid reinforcements suggest further research. The objective is to determine the impact of Hydroxyapatite (HA) and Calcium Silicate (CS) derived from biowaste as hybrid reinforcement in Zn-1Mg-0.2Ti alloy. The influence of hybrid reinforcement (HA&CS) was assessed in various weight percentages. **Methods:** Synthesis of the reinforcement (HA&CS) involved 10h milling and calcination at 1000°C. Pure Zinc and Zn-1Mg-0.2Ti alloy with 5 wt. % and 10 wt. % (HA and CS) biomaterials were fabricated by the squeeze casting process. Hardness tests of the cast samples were conducted with a 1 kg (Hv) force and a 15-second dwell time. The compressive test was performed as per ASTM E9-19, with a ram speed 0.5mm/min. **Findings:** Results suggest that, among all three cases, Zn-1Mg-0.2Ti-(2.5 HA / 2.5 CS) composite exhibited favourable mechanical and microstructural properties. The Zn-1Mg-0.2Ti-(5 HA / 5 CS) composite density was 5.52 kg/m^3, a significant 25% decrease compared to pure zinc metal. The Hardness value of Zn-1Mg-0.2Ti-(2.5 HA / 2.5 CS) was 82Hv, which is 148% increase compared to pure zinc metal (33Hv). The compression tests demonstrated that the Zn-1Mg-0.2Ti-(2.5 HA / 2.5 CS) exhibited the highest ultimate compression strength (364 MPa) and toughness modulus (131 MPa) due to sufficient adherence of the reinforcement with the matrix. **Novelty:** The novelty of the study was to introduce hybrid reinforcements (HA and CS) in the Zn-1Mg-0.2Ti alloy to increase its hardness and compressive strength. Zn-1Mg-0.2Ti-(2.5 HA / 2.5 CS) is a new hybrid composite compared to recent biomaterials. Furthermore, it can be recommended for implants in orthopaedic surgical applications.

Keywords: Zinc Composites; Biodegradable Materials; Hydroxyapatite; Calcium Silicate (Wollastonite); Compressive Strength

1 Introduction

In recent years, biodegradable metals have gained attention, for hard tissue replacement applications, due to their favourable ability to disintegrate slowly under physiological conditions; thereby, revision surgeries caused by implant failures can be avoided. Magnesium (Mg), iron (Fe), and zinc (Zn) have been extensively investigated as recent biomaterials for orthopaedic applications. Compared to Fe-based and Mg-based biomaterials, Zn-based biomaterials exhibit suitable degradation rates without evolving excessive amounts of harmful H_2 gas. In addition, several studies reported that Zn plays several essential biological roles in the human body, such as stimulation of new bone formation, preservation of bone mass, signal transduction, suppression of bone tissue loss and regulation of nucleic acid metabolism. However, Zn, as a pure metal, exhibits insufficient mechanical properties, such as low UTS (20–30 MPa) and hardness (37 Hv)[1]. Therefore, it is unsuitable for most clinical applications, including stents and orthopaedic fixation devices. Furthermore, the relatively low fatigue strength and high susceptibility to the natural ageing of zinc and zinc alloys may result in medical device failure during storage at room temperature (RT) and use in the body. Therefore, the aspects mentioned above are the limitations of the existing approach in developing Zn and Zn alloys before implantation.

Suitable alloying of pure zinc metal with Mg, Ti, Sr, Mn, Li, Fe, and Ag has recently proven to be an effective solution to overcome the issues in zinc alloys[2]. According to a recent report, a Zn-5Mg (5 wt.% Mg) composite achieved an ultimate compressive strength of 256 MPa. Adding magnesium to zinc metal increases its hardness and strength due to the precipitate formation[3]. Li et al. investigated the effect of Ti (titanium) addition in Zn-2Cu-0.01Ti-xLi alloys (x = 0, 0.1 and 0.38). They demonstrated that the addition of Ti shows lamellae of an eutectic mixture of TiZn16 and Zn, which influences the dynamic recrystallization of the Zn grains[4]. Furthermore, metals have relatively low cell adhesion to the surface, which is a crucial factor for synthesising bone-related proteins. One way to address such problems is to combine metals with compounds that improve implant-cell contact, namely bio-ceramics like hydroxyapatite, calcium silicate, bio-glass, and tricalcium phosphate. Around the world, several million metric tons of eggshells are produced daily as biowaste. The eggshell weighs 11% of the egg's total weight and is made of calcium carbonate (94%), organic matter (4%), magnesium carbonate (1%), and calcium phosphate (1%). These are occasionally used as fertilizers due to their high calcium and nitrogen content, but are usually discarded as waste. Eggshells can be used as a natural calcium source in the synthesis of hydroxyapatite. Hydroxyapatite is a bio-ceramic material used in bone replacement applications[5].

Similarly, Rice Husk Ash (RHA) is a by-product of a power plant that uses rice husk as a fuel. Due to environmental dust pollution, the disposal of this waste material poses a hazard. The investigation of RHA as a source of SiO_2 in calcium silicate (wollastonite) preparation for biomaterial application was motivated because of its superior bio-functionalities, excellent biocompatibility, and bioactivity[6]. It is highly appreciated that the existence of these substances dramatically promotes bioactivity and cell proliferation[7]. Zhang et al. reported an adhesive force between the HA/$CaSiO_3$ and Ti; Ti's bioactivity and biocompatibility were improved in the simulated body fluid solution[8]. Another study found that Zn/HA composites exceeded the lower limit for cortical bone and had good mechanical properties for bone replacement[9]. Pathak et al. observed that 3 wt.% of HA in zinc exhibited the maximum compressive yield strength; when HA concentrations increased (9 to 15 wt.%), the compressive yield strength reduced due to the non-diffusion of HA particles [10].

According to the above literature, it is observed that zinc-based biomaterials are emerging biomaterials widely used in bio-medical sectors based on their compatible properties. Furthermore, there is a research gap in using eggshell and rice husk ash (RHA) as initial materials that has to be addressed. Moreover, adding bioceramics as reinforcement in zinc-based biomaterials enhances the bioactivity of the composite. The proposed composite aims to improve the mechanical properties of zinc biomaterial alloys. The novelty in the proposed model is the introduction of suitable alloying elements and biowaste-derived bioactive hybrid reinforcement to effectively increase the strength of zinc biomaterial alloys used in orthopaedic implants. It is essential to assess their physical and mechanical characteristics for their suitability as biomaterials. The present study analyzes the effect of biowaste-derived hydroxyapatite and calcium silicate as reinforcement in biodegradable Zn-Mg-Ti composites fabricated by the squeeze casting process. To the best of the author's knowledge, no study has been conducted on incorporating hybrid ceramic reinforcements in Zn-Mg-Ti biodegradable composites.

2 Methodology

2.1 Zinc, Magnesium and Titanium particles

In the past two decades, research in product development has shown an increasing interest in reducing greenhouse gases, promoting energy conservation, and reducing costs. Magnesium has been developed and has applications in biomedical components and consumer products. Magnesium is 30% less dense than other alloys and 75% less dense than iron-based alloys [3]. Weight reduction is the essence of engineering expertise in developing consumer products, medical applications and aerospace applications. Magnesium, as is well known, is the lightest structural metal available on earth. Magnesium for this research was obtained from Matrics, Nagercoil, India.

Titanium alloys are becoming more and more attractive as high-performance structural materials that are now being used in the biomedical, aerospace and automotive industries owing to their high strength and creep resistance. Titanium alloys have many attractive properties, such as low density and high specific strength. The application of titanium alloys is predicted to multiply, especially in the transport industry. Zinc is a traditional light metal for airborne structures. The family of zinc materials, especially magnesium with titanium cast materials, could be an excellent alternative to steel because of their low density and good strength-to-weight ratio. In this work, the titanium and zinc materials are obtained from Matrics, Nagercoil, India.

2.2 Hydroxyapatite and Calcium silicate (Wollastonite powder)

Materials containing hydroxyapatite are called biomaterials, which possess good cell adhesion. The enhanced mechanical properties, such as modulus, tensile strength, and density of the commonly used biomaterials, can be obtained. Hydroxyapatite synthesized from eggshell and calcium silicate (Wollastonite) powder were selected as the reinforcement. The average grain size of hydroxyapatite is 0.64 μm, and that of calcium silicate is 0.86 μm, which are chosen in this work, respectively. The reinforcements were calculated by weight percentage and ball milled together to make 5- and 10-weight-percent composites containing HA and CS. The powders are mixed in the high energy planetary ball mill (Planetary Mill with TC Balls & Vial, VB Ceramics, Chennai) at 300 rpm with a ball-to-powder ratio standard of 4 for about 10 h to obtain the optimal mixture. The physical and mechanical properties of the precursors used are listed in Table 1. Furthermore, Table 2 illustrates the composition of the specimen and the abbreviations used for convenience in the description.

Table 1. Comparison of physical and mechanical properties of precursors

Materials	ρ (g/cm^3)	CYS (MPa)	Modulus (GPa)	Reference
Pure Zn	7.14	103	2	[1]
Pure Mg	1.71	70	47	[11]
Pure Ti	4.80	250	120	[11]
Hydroxyapatite	2.95	520	115	[12]
Calcium silicate	2.93	250	23	[13]

ρ: density, CYS: Compressive yield strength, UCS: Ultimate compressive strength

Table 2. Specimen Compositions in wt. %

Specimens	HA	CS	Mg	Ti	Zn	Designation
	(All in wt. %)					
Pure Zn	0	0	0	0	100	Pure Zn
Zn-1Mg-0.2Ti- (2.5 HA / 2.5 CS)	2.5	2.5	1	0.2	Balance	ZMT-5R
Zn-1Mg-0.2 Ti- (5 HA/ 5 CS)	5	5	1	0.2	Balance	ZMT-10R

2.3 Fabrication of biomaterial

Squeeze casting is a process suitable for producing metal matrix composites with reinforcements such as whiskers, chopped fibers, and continuous fibers. The Zinc-Magnesium-Titanium-Hydroxyapatite-Calcium Silicate biomaterial was fabricated by using the squeeze casting route. In the current fabrication process, pure zinc ingots, magnesium ingots, and titanium powders were melted in an electric furnace containing a mild steel permanent crucible at a temperature 560ºC. During the preparation process, the crucible was preheated to 100ºC. A gaseous environment consisting of SF_6 (one volume percent) and CO_2 (the balance) was given to protect the molten metal. A stirrer made of stainless steel was used to mix the melt homogeneously at 300 revolutions per minute. The hybrid reinforcement (HA and CS) was milled at 300 rpm in a planetary ball mill. The ball-milled powders were preheated to a 200°C temperature for 10 minutes to increase the wettability with the melt. The liquid metal is poured into a 200°C preheated cylindrical die made of tool steel after the molten metal has been adequately stirred with the reinforcement. The die measures 250 mm in height with an internal diameter of 50 mm. A piston with a diameter of 50 mm was used to apply a squeeze pressure of 100 MPa to the liquid metal. After solidification, the cast part was removed from the die and specimens were prepared for each test. The squeeze casting process and the samples are shown in Figure 2.

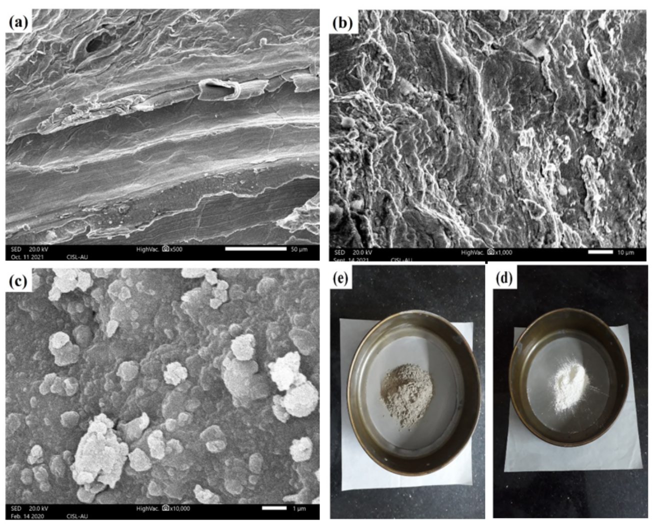

Fig 1. Images of the precursors: (a) Zn, (b) Mg, (c) Ti, (d) Hydroxyapatite, (e) Calcium silicate

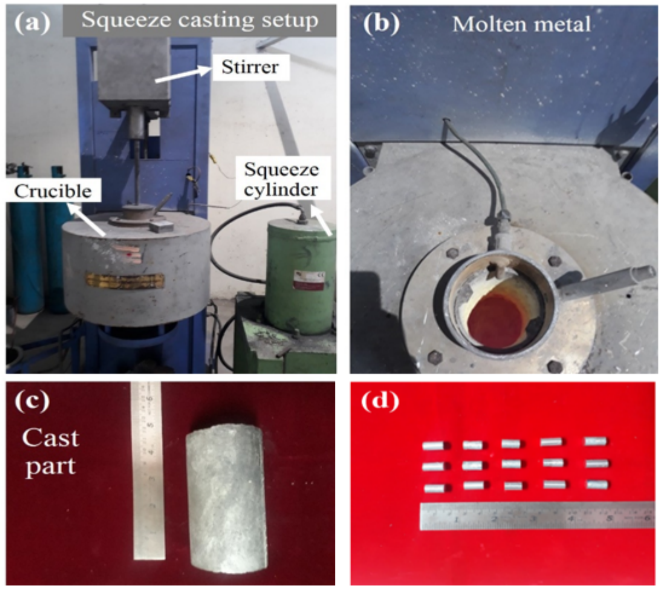

Fig 2. Fabrication details of composites: (a) Squeeze casting setup, (b) Molten metal in the crucible, (c) Solidified cast component, (d) Test specimens

2.4 Characterizations

2.4.1 Density and porosity

Density measurement was performed using the Archimedes principle as per ASTM B962-13, as shown in Equation 1, where m_s the mass of the saturated sample, m_d is the mass of a dry sample, m_{susp} is the mass of a suspended sample, and ρ_{H_2O} is the density of water. The porosity (P) is calculated by using Equation 2

$$\rho_{\text{composite}} = \frac{m_d}{m_s - m_{su\ sp}} \times \rho_{H_2O} \tag{1}$$

$$P = \frac{m_s - m_d}{m_s - m_{su\ sp}} \times 100\% \tag{2}$$

2.4.2 Micro Hardness

The Vickers microhardness testing machine (Zwick Roell, Germany) was used to measure the resistance to indentation. Before conducting the hardness test, emery paper was used to polish both sides of the specimens to achieve uniform load distribution. The experiment was conducted with a 1 kg (Hv) force and a 15-second dwell time per ASTM E384 – 17 standards. Three different places were pointed for each test, and an average value was considered.

2.4.3 Compression strength

The compression strength was measured using a universal testing machine (Unitek 9400, India) as per the ASTM E9-19 Standard. The mean of three samples was considered. The dimensions of each sample are chosen as 10 mm in diameter and 15 mm in height, with a ram speed of 0.5 mm per minute. Each test was conducted in a laboratory environment at ambient conditions.

2.4.4 Microstructure characterisation

The morphology of the specimens was examined using a scanning electron microscope (SEM: JEOL-JSM - IT 200, Japan) as per the ASTM E407 standard. The specimens were ground before the microstructure analysis with P320-P2000 sandpaper and 1 μm diamond paste. An alcohol solution containing 0.5% HNO_3 was used as an etchant.

2.4.5 Phase characterisation

The phase analysis of the samples was examined using an X-ray diffractometer (Rigaku, Miniflex 600, Japan, Cu K = 0.15406 nm). All the measurements were performed at room temperature, in Bragg-Brentano geometry, with a 0.02° step size throughout an angular range of 2θ = 20–80°. Phases were identified with standards documented by the Joint Committee on Powder Diffraction Standards (JCPDS).

3 Results and Discussion

3.1 Density and Porosity Analysis

A density study of pure Zn metal and ZMT alloy reinforced with HA and CS is illustrated in Figure 3 (a). The density of pure zinc metal was 7.05 kg/m^3. In contrast, the ZMT–5R and ZMT–10 R composite densities were 5.73 kg/m^3 and 5.52 kg/m^3, respectively. The density measurement shows a decreasing trend with an increase in HA and CS reinforcement concentration in the ZMT alloy. In contrast, the porosity increases as the reinforcement concentration increases. This behaviour could be due to the addition of less dense reinforcement to a denser matrix phase. It should be noted that the increase in porosity shown in Figure 3 (b) is advantageous to osteoblast formation in implants, and hydroxyapatite has excellent biocompatibility. Due to its low density, HA has an extremely high strength-to-weight ratio, which makes it suited for biomaterial applications.

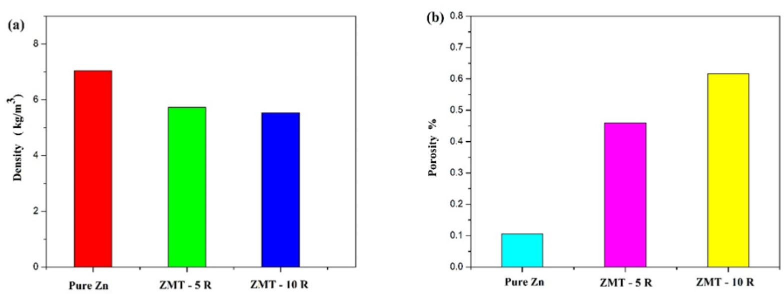

Fig 3. (a) Density and (b) Porosity of Pure Zn, ZMT – 5R, and ZMT – 10 R

3.2 Hardness test

The hardness measurement of pure zinc and the ZMT alloy reinforced with HA and CS is shown in Figure 4. A significant 148 % increased hardness was observed in the ZMT–5R composite (82 Hv) compared to pure Zn (33 Hv). The intermetallic precipitates that formed along the grain boundaries and the presence of hard bioactive ceramics in the composite are the causes of this behavior. Further, increase in reinforcement (HA and CS combined) to 10 wt. % in the ZMT-10R (69 Hv) composite resulted in a 15 % reduction compared to the ZMT–5R composite, as shown in Figure 3. The decrement in hardness value in ZMT–10 R composite can be related to the phenomenon that whenever a higher concentration of reinforcement is added to the matrix, the reinforcement themselves adhere together due to high volume and detach from the matrix, resulting in weak mechanical properties of the composite. The above behaviour correlates well with Pinc et al.'s findings[9]. They evaluated the mechanical properties of Zn-HA biomaterials at different weight fractions of 1% to 10%. Their study found that improved mechanical properties were observed while increasing the weight fraction of HA compared to pure zinc metal.

3.3 Compression test analysis

The stress-strain curves obtained from the compressive strength of pure zinc and the ZMT alloy reinforced with HA and CS are shown in Figure 5. Their significant values are represented in Figure 6. As can be seen from Figure 5, Pure Zn did not show any critical points of significance. On the other hand, the stress-strain plot of the ZMT–5 R and ZMT–10 R composite represented a typical stress-strain plot. The corresponding changes in the composites compared to pure Zn may be attributed to the alloying and reinforcement element properties. Since there was no appreciable yield behaviour in the stress-strain curve of the samples, the yield stress was found from the offset method. The compressive yield stresses (CYS) obtained were 240 MPa, 180 MPa, and 125 MPa for pure Zn, ZMT-5 R, and ZMT-10 R composites, respectively. The reduction in yield stress of the composites ZMT

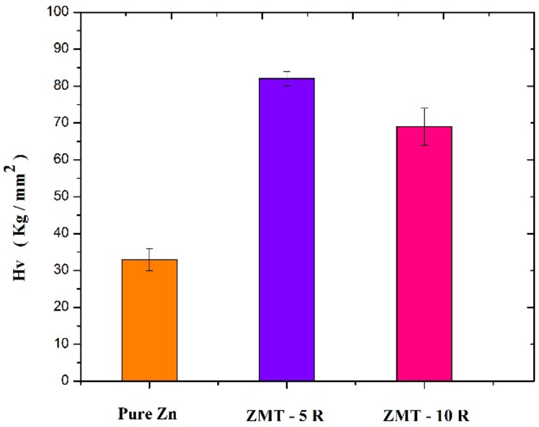

Fig 4. Hardness variation of Pure Zn, ZMT – 5R, and ZMT – 10 R

–5 R and ZMT–10 R is attributed to the addition of ceramics. The ultimate compressive stress (UCS) obtained from ZMT–5 R (364MPa) was higher than ZMT – 10 R and Pure Zn. The UCS value of ZMT-10 R is comparable to the compressive strength of cortical bone (230 MPa). The ZMT–5 R exhibited the highest toughness modulus among all three samples at 131 MPa. The reason for this behaviour may be attributed to the optimum concentration of reinforcement. Adherence of the reinforcement phase to the matrix phase depends on the reinforcement concentration[14]. However, crack deflection may be the primary mechanism for toughening HA particles in the matrix. Table 2 indicates the mechanical properties of various biomaterials and human bone compared with the prepared composite. ZMT–5 R composite has higher mechanical properties than cortical bone and recently developed composites.

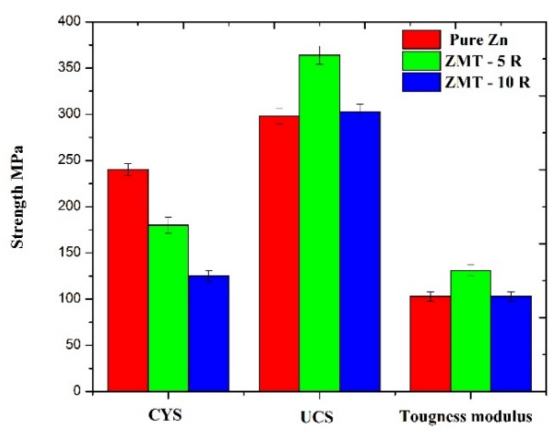

Fig 5. Stress - strain curve of Pure Zn, ZMT – 5R, and ZMT – 10 R

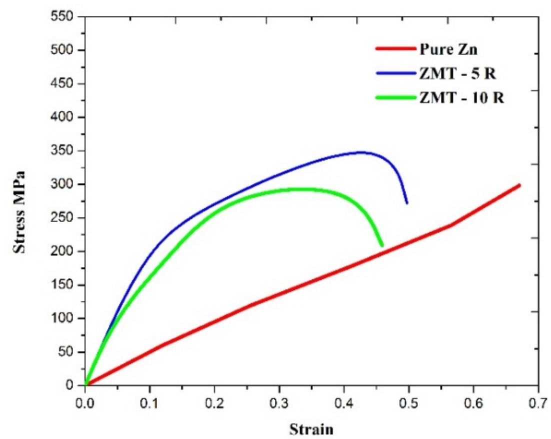

Fig 6. CYS, UCS and toughness modulus of Pure Zn, ZMT – 5R, and ZMT – 10 R

Table 3. Overview of mechanical properties of selected biomaterial and human bone

Materials	Hardness (Hv)	CYS(MPa)	UCS(MPa)	Reference
Cortical bone	-	-	88-230	[9]
Cancellous bone	-	-	0.2-80	[9]
PM zinc	33	81	-	[9]
Zn / 16 HA	24	46	65	[9]
ZMT-5 R	82	180	364	This study

3.4 Investigation of XRD analysis

The XRD results on the plane of diffraction of pure zinc and the ZMT alloy reinforced with HA and CS are shown in Figure 7. The high-intensity individual isolated peaks with a plane of diffraction obtained for pure Zn(JCPDS # 04-0831), as shown in Figure 7 a. represent the metal's purity by crystalline homogeneity.

The peaks associated with the $Zn_{16}Ti$ (JCPDS # 41-1283) intermetallic phase were caused by the α–Zn matrix and the presence of Ti, as shown in Figure 7 b. In addition, the intermetallics $Zn_{11}Mg_2$ (JCPDS # 06-0664) associated with the α–Zn matrix and Mg is shown in Figure 7 b. The minor peaks in Figure 7 b and Figure 7 c represent Zn, Mg, and Ti elements in their formative stage. The formation of HA (JCPDS# 9-432) and CS(JCPDS # 29-0369) compounds with zinc was also observed. Based on the XRD results with unique and independent peaks, it could be stated that the phase purity obtained in the composite preparation is very high, which would be advantageous in implant materials.

3.5 Microstructure analysis

Figure 8 (a-b) depicts the typical SEM morphology of pure zinc metal. It is evident from the microstructure images represented in Figure 8a that pure zinc has a fibrous morphology responsible for its ductility property. Specifically, the yield strength of the material is highly influenced by the morphology of the microstructure obtained after the solidification process. Furthermore, the tangled fibrous morphology forms a cluster zone pattern, which would benefit osteoblast adhesion by bioactive ceramics reinforced in biomaterial composites used for implant applications. The primary reasons for the represented morphology may be the formation of large grains and homogeneity.

Additionally, Figure 8 (a-b) shows multiple lamellae and globules. The reason could be the influence of varying cooling zones along the cast part. During the solidification process, the grain growth near the die wall zone differs from the grain growth in the central regions of the casting. As a result, multiple morphologies can be seen in Figure 8 (a-b). Moreover, fibrous morphology ensures that the ductility is not affected by variations in the cooling zones during the solidification process. The density, pores, and pore connectivity greatly influence the mechanical properties of the materials. Minimal cracks and pores in the microstructure can be attributed to the high density of pure zinc metal. Density plays a vital role in releasing the gases

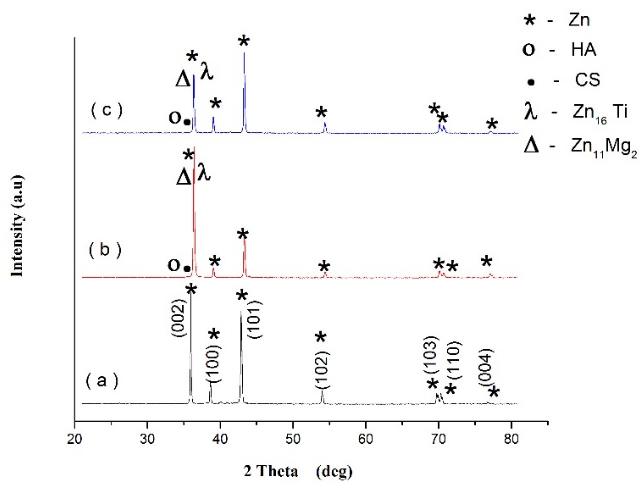

Fig 7. XRD plots (a) Pure Zn, (b) ZMT – 5R, (c) ZMT – 10 R

formed during casting and solidification.

Figure 9 (a-b) shows the SEM morphology of the ZMT-5 R composite. The hybrid ceramic reinforcement (each 2.5wt.%-HA and CS) in the ZMT alloy can be seen along the grain boundaries. The intermetallic precipitates along the grain boundaries aid the hybrid ceramic reinforcement to be distributed homogeneously, which could improve the mechanical properties profoundly. Zinc with titanium particles forms the $Zn_{16}Ti$ intermetallic precipitates. Specifically, the intermetallic precipitates improve the mechanical properties of the composites. The precipitates on the grain boundaries of α-Zn grains disperse as the melt undergoes an eutectic reaction (L-Zn+$Zn_{16}Ti$)[15] . The cracks observed in Figure 8 a can be attributed to the hybrid ceramic reinforcement in the ZMT–5 R composite. From Figure 8 b, a non-uniform coarse morphology in $Zn_{16}Ti$ is observed. Similarly, from Figure 8 b, the morphology of $Zn_{11}Mg_2$ is evidenced as needle a morphology based on the eutectic reaction between zinc and magnesium[16] . Figure 8 a and b exhibit a homogeneous distribution of the precipitates along with the reinforcement HA and CS along the grain boundaries. The homogeneity in distribution can be attributed to the sufficient concentration of the reinforcement responsible for self-alignment along the boundaries.

Figure 10 a and b show the SEM morphology of the ZMT-10 R composite, in which 5 wt.% of HA and 5 wt.% of CS are incorporated. As shown in Figure 9 a, the precipitate stack and the reinforcement separated themselves, forming reinforcement agglomerations randomly. Individual agglomeration globules can be seen in both Figure 10 a and b. Furthermore, reinforcement was partially fused to the precipitates, as shown in Figure 10 b. This phenomenon can be attributed to the high reinforcement concentration. The agglomerations of HA influence the mechanical and degradation properties of the composites[17] .

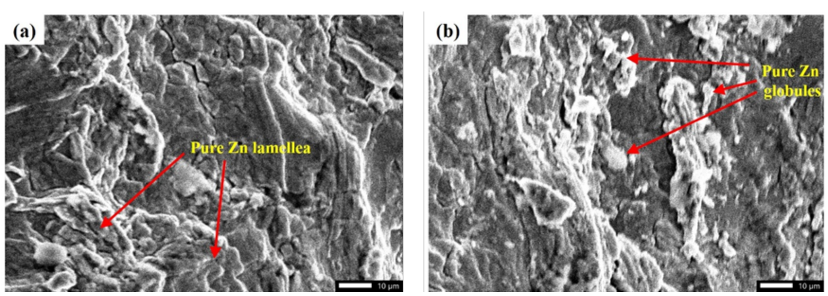

Fig 8. SEM morphology of pure Zn

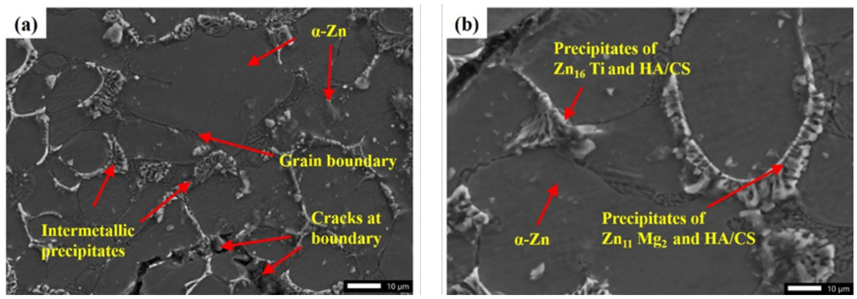

Fig 9. SEM morphology of ZMT – 5 R

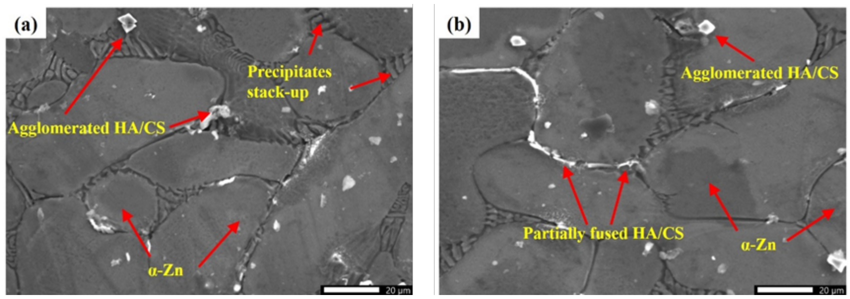

Fig 10. SEM morphology of ZMT – 10 R

4 Conclusion

In this research work, zinc biomaterials were developed with biowaste derived hydroxyapatite and calcium silicate and their suitability was assessed based on their physical, mechanical and microstructural characteristics. Following are the conclusions drawn as a result of the characterisation:

1. The density of the 10% hybrid reinforced composite was 5.52 kg/m^3, which is 25% less than the density of pure zinc metal.
2. When the hybrid reinforcement was increased to 5%, the hardness increased by 148% (82 Hv) compared to pure Zn.
3. The ultimate compressive strength of 5 % hybrid reinforced composite was reported to be 364 MPa, which is higher than pure Zn and cortical bone (230MPa).
4. The highest toughness modulus (131 MPa) was achieved when the hybrid reinforcement was increased to 5% when compared to pure Zn and 10 % hybrid reinforced composites due to sufficient adherence of the reinforcement with the matrix.
5. Microstructural examination showed the presence of $Zn_{16}Ti$ intermetallic precipitate with a non-uniform, coarse-grouped morphology and $Zn_{11}Mg_2$ with an ordered, needle-like morphology.

The overall characteristics of these composites indicate that they could be used as an alternative biomaterial in orthopedic applications, which require superior physical and mechanical properties compared to the recently identified unreinforced Zn-Mg and Zn-Ti binary alloys. In the coming years, scientists and researchers could use the results of this study to do more research on biomaterials to address orthopedic issues due to aging and injuries.

References

1) Hernández-Escobar D, Champagne S, Yilmazer H, Dikici B, Boehlert CJ, Hermawan H. Current status and perspectives of zinc-based absorbable alloys for biomedical applications. *Acta Biomaterialia*. 2019;97:1–22. Available from: https://doi.org/10.1016/j.actbio.2019.07.034.
2) Kabir H, Munir K, Wen C, Li Y. Recent research and progress of biodegradable zinc alloys and composites for biomedical applications: Biomechanical and biocorrosion perspectives. *Bioactive Materials*. 2021;6(3):836–879. Available from: https://doi.org/10.1016/j.bioactmat.2020.09.013.
3) Pachla W, Przybysz S, Jarzębska A, Bieda M, Sztwiertnia K, Kulczyk M, et al. Structural and mechanical aspects of hypoeutectic Zn–Mg binary alloys for biodegradable vascular stent applications. *Bioactive Materials*. 2021;6(1):26–44. Available from: https://doi.org/10.1016/j.bioactmat.2020.07.004.
4) Li L, Liu C, Jiao H, Yang L, Cao F, Wang X, et al. Investigation on microstructures, mechanical properties and in vitro corrosion behavior of novel biodegradable Zn-2Cu-0.01Ti-xLi alloys. *Journal of Alloys and Compounds*. 2021;888:161529. Available from: https://doi.org/10.1016/j.jallcom.2021.161529.

5) Puad NASM, Koshy P, Abdullah HZ, Idris MI, Lee TC. Syntheses of hydroxyapatite from natural sources. *Heliyon*. 2019;5(5):e01588. Available from: https://doi.org/10.1016/j.heliyon.2019.e01588.
6) Palakurthy S, K VGR, Samudrala RK, P AA. In vitro bioactivity and degradation behaviour of β-wollastonite derived from natural waste. *Materials Science and Engineering: C*. 2019;98:109–117. Available from: https://doi.org/10.1016/j.msec.2018.12.101.
7) Mathina M, Shinyjoy E, Kavitha L, Gopi D. Biowaste-derived hydroxyapatite reinforced with polyvinyl pyrrolidone/aloevera composite for biomedical applications. *International Journal of Applied Ceramic Technology*. 2021;18(1):221–234. Available from: https://doi.org/10.1111/ijac.13630.
8) Zhang L. Surface Modification of Titanium by Hydroxyapatite/CaSiO3/Chitosan Porous Bioceramic Coating. *International Journal of Electrochemical Science*. 2020;15:3616–3626. Available from: https://doi.org/10.20964/2020.04.08.
9) Pinc J, Čapek J, Kubásek J, Průša F, Hybášek V, Veřtát P, et al. Characterization of a Zn-Ca5(PO4)3(OH) Composite with a High Content of the Hydroxyapatite Particles Prepared by the Spark Plasma Sintering Process. *Metals*. 2020;10(3):372. Available from: https://doi.org/10.3390/met10030372.
10) Pathak DK, Pandey PM. An experimental investigation of the fabrication of biodegradable zinc–hydroxyapatite composite material using microwave sintering. *Proceedings of the Institution of Mechanical Engineers, Part C: Journal of Mechanical Engineering Science*. 2020;234(14):2863–2880. Available from: https://doi.org/10.1177/0954406220910445.
11) Seetharaman S, Subramanian J, Singh RA, Wong WLE, Nai MLS, Gupta M. Mechanical Properties of Sustainable Metal Matrix Composites: A Review on the Role of Green Reinforcements and Processing Methods. *Technologies*. 2022;10(1):32–32. Available from: https://doi.org/10.3390/technologies10010032.
12) Pal A, Metya AK, Chowdhury AR, Sinha A. Structural and Mechanical Behavior of Mechanochemically Synthesized Nanocrystalline Hydroxyapatite from Mercenaria Clam Shells. *Transactions of the Indian Ceramic Society*. 2020;79(4):175–181. Available from: https://doi.org/10.1080/0371750X.2020.1792806.
13) Shanmuganantha L, Baharudin A, Sulong AB, Shamsudin R, Ng MH. Prospect of Metal Ceramic (Titanium-Wollastonite) Composite as Permanent Bone Implants: A Narrative Review. *Materials*. 2021;14(2):277. Available from: https://doi.org/10.3390/ma14020277.
14) Kubásek J, Dvorský D, Čapek J, Pinc J, Vojtěch D. Zn-Mg Biodegradable Composite: Novel Material with Tailored Mechanical and Corrosion Properties. *Materials*. 2019;12(23):3930. Available from: https://doi.org/10.3390/ma12233930.
15) Wang K, Tong X, Lin J, Wei A, Li Y, Dargusch M, et al. Binary Zn–Ti alloys for orthopedic applications: Corrosion and degradation behaviors, friction and wear performance, and cytotoxicity. *Journal of Materials Science & Technology*. 2021;74:216–229. Available from: https://doi.org/10.1016/j.jmst.2020.10.031.
16) Zhang S, Yuan P, Wang X, Wang T, Zhao L, Cui C. Fabrication and Properties of Zn-3Mg-1Ti Alloy as a Potential Biodegradable Implant Material. *Materials*. 2022;15(3):940. Available from: https://doi.org/10.3390/ma15030940.
17) Hosová K, Pinc J, Školáková A, Bartůněk V, Veřtát P, Školáková T, et al. Influence of Ceramic Particles Character on Resulted Properties of Zinc-Hydroxyapatite/Monetite Composites. *Metals*. 2021;11(3):499. Available from: https://doi.org/10.3390/met11030499.